

The Role of Adventitious Carbon in Photo-catalytic Nitrogen Fixation by Titania

Benjamin M. Comer,[†] Yu-Hsuan Liu,[‡] Marm B. Dixit,[⊥] Kelsey B. Hatzell,[⊥] Yifan Ye,[§]
Ethan J. Crumlin,[§] Marta C. Hatzell,^{*,||} and Andrew J. Medford^{*,†}

[†]School of Chemical & Biomolecular Engineering, Georgia Institute of Technology, Atlanta, Georgia 30318, United States

[‡]School of Civil and Environmental Engineering, Georgia Institute of Technology, Atlanta, Georgia 30313, United States

[⊥]Department of Mechanical Engineering, Vanderbilt University, Nashville, Tennessee 37235, United States

[§]Advanced Light Source, Lawrence Berkeley National Laboratory, Berkeley, California 94720, United States

^{||}George W. Woodruff School of Mechanical Engineering, Georgia Institute of Technology, Atlanta, Georgia 30313, United States

ABSTRACT: Photo-catalytic fixation of nitrogen by titania catalysts at ambient conditions has been reported for decades, yet the active site capable of adsorbing an inert N₂ molecule at ambient pressure and the mechanism of dissociating the strong dinitrogen triple bond at room temperature remain unknown. In this work in situ near-ambient-pressure X-ray photo-electron spectroscopy and density functional theory calculations are used to probe the active state of the rutile (110) surface. The experimental results indicate that photon-driven interaction of N₂ and TiO₂ is observed only if adventitious surface carbon is present, and computational results show a remarkably strong interaction between N₂ and carbon substitution (C*) sites that act as surface-bound carbon radicals. A carbon-assisted nitrogen reduction mechanism is proposed and shown to be thermodynamically feasible.

The findings provide a molecular-scale explanation for the long-standing mystery of photo-catalytic nitrogen fixation on titania. The results suggest that controlling and characterizing carbon-based active sites may provide a route to engineering more efficient photo(electro)-catalysts and improving experimental reproducibility.

Photo(electro)-catalytic nitrogen fixation presents an exciting route toward ammonia production at benign conditions.^{1,2} Photon-driven nitrogen reduction and oxidation have been reported over numerous semiconductors, with titania-based catalysts being the most common.^{1,3,4} The hypothesis that nitrogen fixation on titania occurs via photo-catalytic reactions of hydrocarbons was first proposed over 75 years ago by Dhar et al. on the basis of illuminated compost experiments.⁵ Photo-generation of ammonia by titania-based catalysts has been reported by numerous independent groups since, including with more controlled techniques such as isotopic labeling;^{3,6,7} however, the influence of hydrocarbons was neglected. There are also considerable discrepancies in the literature and open questions regarding the thermodynamics that drive the process.^{1,8,9} Given the recent explosion of interest in this field,¹ it is critical to establish hypotheses about the

active site and reaction mechanism that resolve these inconsistencies.⁸

The prevailing hypothesis is that oxygen defects are the active sites for nitrogen fixation,^{7,10,11} based primarily on an observed correlation between oxygen defect density and ammonia yields.^{7,10} However, the alignment of the conduction band edge relative to the N₂/NH₃ redox couple provides a relatively small driving force, equivalent to an overpotential of only 0.15 V.⁹ Density functional theory (DFT) calculations have shown that the bridging oxygen (O-br) vacancy of rutile (110) exhibits weak N₂ adsorption energy (0.2 eV uphill) and requires substantially larger overpotentials (>1.5 V).^{9,12} One alternative hypothesis is that oxidative processes drive nitrogen fixation due to the substantially larger electrochemical driving force from photo-generated holes.^{9,13} However, adsorption of N₂ is still required, and nitrate products have rarely been reported.¹³ This indicates that other mechanisms are likely involved.

In this work, direct insight into the nature of the active state of titania is obtained using near-ambient-pressure X-ray photo-electron spectroscopy (AP-XPS) experiments. A rutile (110) model surface is chosen based on the observation that ammonia yields correlate with the amount of rutile.⁴ The experiments are conducted in the absence of light and with in situ illumination (Figure 1) with ultraviolet/visible light at a temperature of 200 °C. The sample is exposed to 300 mTorr of N₂ both with and without illumination. The results for the as-prepared rutile (110) crystal (Figure 1a,b) indicate the emergence of a peak at 398 eV in the N 1s spectrum upon illumination (Figure 1b). This value has previously been attributed to reduced nitrogen N_{red} (NH₃ = 398.8 eV).^{14–16} No changes in the binding energy of Ti 2p_{3/2} or Ti 2p_{1/2} are observed with the addition of N_{red} (Tables S1–S4), indicating that the reduced nitrogen on the surface does not change the titania crystal structure through surface nitride formation.¹⁵ Furthermore, repeated experiments at lower temperatures of 35 and 100 °C (Figure S2) reveal that reduced nitrogen species remain on the surface in the dark at low temperatures, indicating that they are adsorbed. These results provide strong direct evidence of a photo-induced interaction between the titania surface and nitrogen.

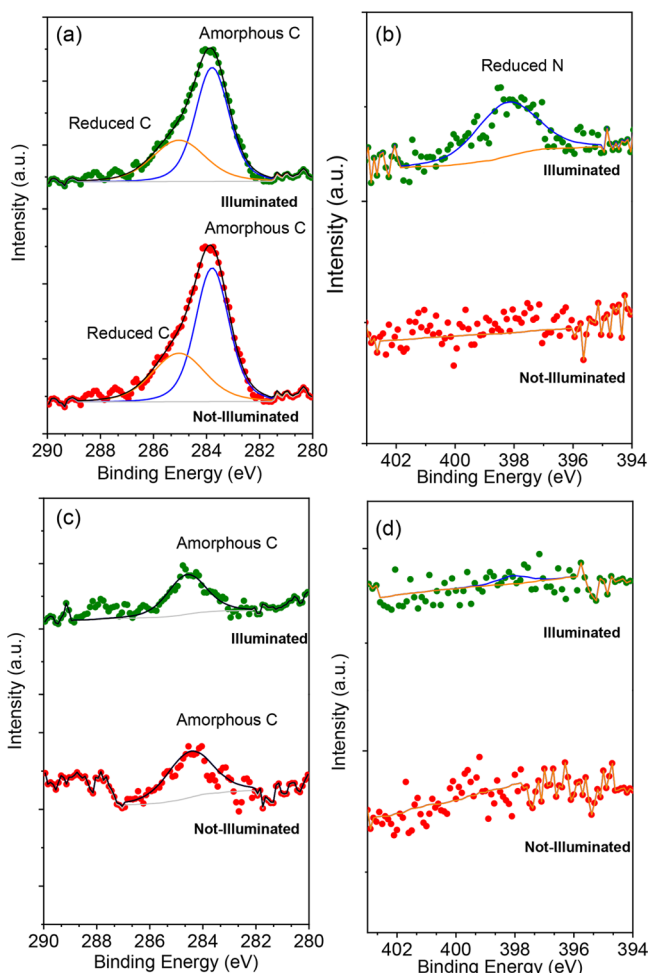


Figure 1. Results of in situ AP-XPS on rutile (110) single crystal with C 1s (a,c) and N 1s (b,d) peaks for the as-received (a,b) and cleaned (c,d) surfaces in the dark (red) and under visible illumination (green) when exposed to 300 mTorr nitrogen.

The AP-XPS results also indicate that adventitious carbon is present on the sample (Figure 1a), a result typical for titania.^{17,18} However, oxygen vacancies are not detected, as evidenced by the sharp the Ti 2p_{3/2} peak (Figure S1) that indicates all Ti⁴⁺ sites are well coordinated.¹⁹ The adventitious carbon is removed from the sample by annealing at 500 °C in 100 mTorr O₂ for 90 min, resulting in a substantial reduction in the C 1s peak intensity and likely oxidation of surface hydrocarbons. After this cleaning procedure the N 1s peak is no longer detected upon illumination. To confirm that the disappearance of the photo-induced N 1s peak is not due to annealing of oxygen defects a second experiment was performed in which oxygen defects are introduced via Ar⁺ sputtering.²⁰ Sputtering the sample simultaneously removes a portion of the adventitious carbon. The presence of oxygen vacancies is confirmed by the appearance a shoulder in the Ti 2p spectra; however, the introduction of oxygen vacancies does not result in a greater reduced nitrogen peak (Figure S3). The defects are then partially healed through the introduction of CO₂ and N₂, followed by CO₂, N₂, and H₂O. The addition of CO₂ resulted in increased C 1s and N_{red} peaks (Figure S3), providing additional evidence of the interaction between surface carbon and nitrogen. This finding also indicates that

oxygen vacancies may play an indirect role by favoring formation of surface carbon.

The atomic-scale structure of adventitious surface carbon is not well defined,²¹ and an ensemble of active-site structures are likely to contribute. To address this challenge the N₂ binding energy and surface energy of a large swath of active sites are calculated using DFT with the BEEF-vdW functional (see Supporting Information (SI)). These sites include a range of oxygen/titanium defects and carbon additions/substitutions on the rutile TiO₂ (110) surface. The results, shown in Figure 2,

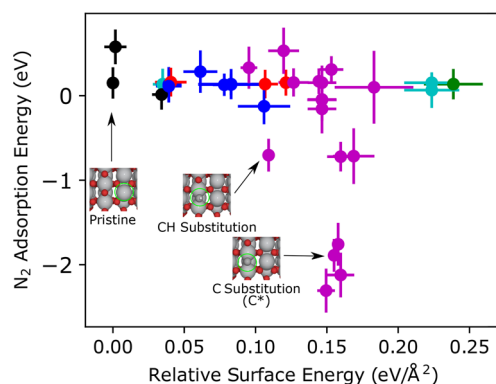


Figure 2. Surface formation energy of various surface models vs the adsorption energy of N₂ evaluated at 0 V RHE relative to pristine rutile (110), bulk TiO₂, and graphite. Site classes include stoichiometric TiO₂ (black), O vacancies (blue), carbon additions (red), Ti additions (green), Ti addition and carbon (cyan), and O vacancies with carbon (magenta).

illustrate a trade-off of reactivity and stability, where the most relevant sites exhibit maximum stability for a given N₂ adsorption energy.²² There are several carbon-based active sites that exhibit remarkable N₂ adsorption free energies of ~2 eV, providing further theoretical support for the hypothesis that adventitious carbon enables interaction between TiO₂ and N₂. In addition to strong binding, it is necessary that N₂ adsorption be selective against other reactants, that active sites are sufficiently stable to exist under reaction conditions, and that a catalytic mechanism for N–N bond scission exists. We select a single representative active site, a carbon substitution at a bridging oxygen (C*), as a model to investigate these issues.

The C* site has a remarkably strong N₂ binding free energy of -1.89 eV, equivalent to the gas-phase analogue of the reaction (C+N₂ → CN₂). This equivalence indicates that the C* site acts as a surface-bound carbon radical, which is corroborated by two unpaired electrons in the surface slab and a magnetic dipole of 1.56 μ_B on the C atom. This reactive carbon radical can also interact with other species under reaction conditions. The presence of H₂O is required for proton formation via oxygen evolution, and O₂ is also present in many studies. The adsorption selectivity toward N₂ is assessed by computing the free energy of adsorption for H₂O and O₂ as a function of O₂ chemical potential at ambient temperature and pressure (300 K, 1 bar) and 100% humidity (Figure 3); the BEEF-vdW ensemble is used to propagate DFT error and compute surface coverage probabilities (see SI). The results illustrate that N₂ adsorption is competitive within the error of DFT, and that N₂ adsorption will be favored by decreasing O₂ pressure. This is consistent with the observation that anaerobic conditions increase reaction rates.⁷ These results support the

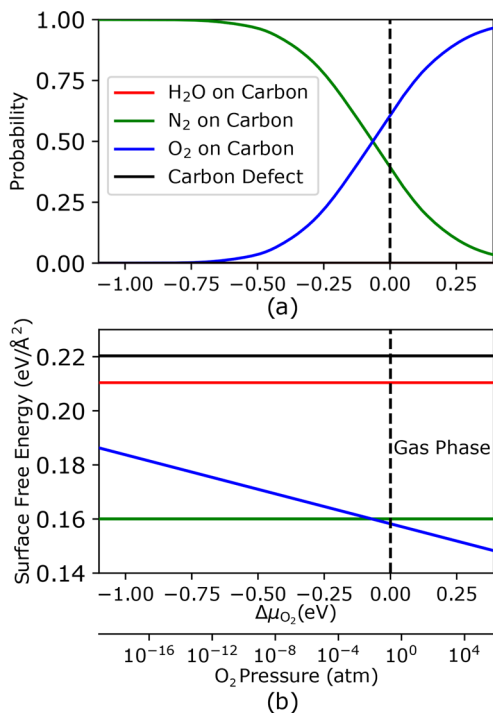


Figure 3. (a) Probability of each reactant species being dominant on the C* site based on uncertainty propagation from BEEF-vdW DFT calculations. (b) Surface energy of each reactant species at different O₂ chemical potentials. All chemical potentials are evaluated at 300 K. The reference chemical potential (0 eV) corresponds to 0.2 atm of O₂, 0.8 atm of N₂, and 0.035 atm of H₂O (100% RH).

hypothesis that C* and other carbon-based sites enable selective adsorption of N₂ at ambient conditions.

The carbon-based active sites show a clear trend toward strong N₂ adsorption but are also relatively unstable (Figure 2), raising the question of whether they exist in a real system. The surface energies shown in Figure 2 are computed relative to graphite, one of the most stable forms of carbon. Adventitious surface carbon will be less stable, and likely consists of a variety of short-chain hydrocarbons and carbon oxides.²¹ The photocatalytic activity of TiO₂ for hydrocarbon oxidation and CO₂ reduction is well established^{23,24} suggesting that the carbon site may be formed by a photo-oxidation/reduction. Adventitious carbon has also been reported to play a role in photo-catalytic

CO₂ reduction,¹⁸ and hydrocarbon-based sacrificial reagents have been shown to increase ammonia yields.^{6,25,26} We model the hydrocarbon influence by selecting CH₄ as a representative hydrocarbon. Any alcohol or short-chain hydrocarbon on the surface will be thermodynamically easier to oxidize. The photochemical oxidation is modeled using the computational hydrogen electrode (CHE),²⁷ and an O-br vacancy is used as the active site such that the adsorbed C* is equivalent to the bridging carbon substitution. The results show that photo-oxidation of CH₄ to the C* site is highly exothermic (Figure 4a) owing to the strong oxidative potential of photo-generated holes. This is clear from the band alignment of TiO₂ where there is a thermodynamic driving force of >1 eV even for the formation of gas-phase C atoms from CH₄. This is also consistent with experimental observation of CH_x surface species, including radicals, on titania.^{28–30} These findings provide strong evidence that the formation of metastable carbon active sites on titania is feasible under photo-catalytic conditions.

Finally, adsorption of N₂ is only the first step in the formation of ammonia; the challenge of dissociating the N–N bond still remains. The feasibility of the ammonia synthesis half-reaction on the C* site was mapped out following a range of possible reaction mechanisms (see SI). The CHE approximation is used, and only thermodynamics of intermediate states are considered. The most favorable route follows the distal mechanism of N–N bond scission,³¹ and exhibits a low thermodynamic barrier of 0.55 ± 0.12 eV with the potential-limiting step being the hydrogenation of CN* (Figure 4c). The formation of the second NH₃ requires hydrogenation of both the C and N in order to weaken the C–N bond (Figures S4 and S5) resulting in a surface CH₃*, which must be regenerated via photo-oxidation in order to close the catalytic cycle (Figure 4b). While kinetic limitations have been neglected, the results show that carbon-based active sites provide a thermodynamically feasible route to photo-catalytic nitrogen fixation on titania catalysts.

The proposed mechanism explains how photo-catalytic reduction of nitrogen to ammonia can occur despite the relatively small reductive driving force from the TiO₂ conduction band edge. The oxidative potential of photo-generated holes is captured by the formation of metastable reactive carbon species that promote strong N₂ bonding and subsequent reduction via surface-bound CN₂H_x species. This is similar to the well-known role of photo-generated O₂^{•-} and

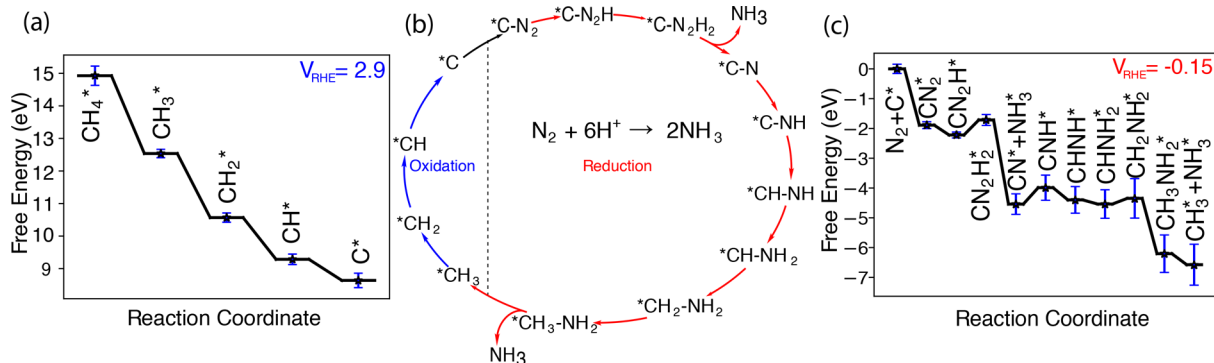


Figure 4. (a) Free energy diagram of the oxidative active site regeneration. The potential is set to that of oxidizing holes at the band edge of rutile TiO₂. (b) Thermodynamic cycle of N₂ reduction on a carbon substitution at a bridging oxygen (C*) on TiO₂. The path consists of a reductive portion (red) and an oxidative active site regeneration portion (blue). (c) Free energy diagram of the reductive ammonia production portion of the thermodynamic cycle. The potential is set to that of reducing electrons at the band edge of rutile TiO₂.

OH[•] radicals in TiO₂ photo-oxidation.³² The proposed hypothesis also explains numerous prior experimental observations and inconsistencies: rates correlate with oxygen vacancies because they promote the formation of reactive carbon sites, the rate of ammonia formation decreases with oxygen concentration due to poisoning of N₂ adsorption sites, and the wide range of experimentally observed rates is due to the lack of effort to control or characterize carbon-based impurities on the catalyst surface or reaction environment.

In conclusion, a combination of AP-XPS experiments and DFT studies provide strong experimental and theoretical support for the hypothesis that adventitious surface carbon promotes photo-induced adsorption of N₂ at TiO₂ through the formation of metastable active sites by photo-oxidation of hydrocarbon species. The DFT results indicate that carbon-based sites interact strongly with N₂, and that subsequent reductive hydrogenation of CN₂ is a thermodynamically feasible route to produce ammonia and regenerate the surface hydrocarbon. This hypothesis is consistent with prior reports of carbon radical formation,^{28–30} the role of surface carbon contaminants in photo-catalysis,¹⁸ spin-mediated N₂ adsorption,³³ and strong interactions between nitrogen and graphene edges.³⁴ The hypothesis is also consistent with a number of key observations in the nitrogen photo-fixation literature including the correlation of rate with oxygen vacancies^{7,10} and sacrificial reagents,^{6,25,26} the detrimental effect of gas-phase oxygen,⁷ and the large variations and inconsistencies in measured rates for catalysts that are nominally identical.^{1,7,8} The findings indicate that careful characterization and control of surface carbon is critical to ensure reproducibility in photo-catalytic nitrogen fixation on titania and other semiconductors, and suggest that engineering carbon-based active sites is a promising strategy for enhancing photo-catalytic nitrogen fixation.

AUTHOR INFORMATION

Corresponding Authors

*marta.hatzell@me.gatech.edu

*andrew.medford@chbe.gatech.edu

ORCID

Kelsey B. Hatzell: 0000-0002-5222-7288

Ethan J. Crumlin: 0000-0003-3132-190X

Marta C. Hatzell: 0000-0002-5144-4969

Andrew J. Medford: 0000-0001-8311-9581

Notes

The authors declare no competing financial interest.

ACKNOWLEDGMENTS

This research used resources of the Advanced Light Source, which is a DOE Office of Science User Facility under contract no. DE-AC02-05CH11231. A.J.M. and M.C.H. are grateful to J. G. Edwards for constructive discussions and suggestions.

REFERENCES

- (1) Medford, A. J.; Hatzell, M. C. *ACS Catal.* **2017**, *7*, 2624–2643.
- (2) Shipman, M. A.; Symes, M. D. *Catal. Today* **2017**, *286*, 57–68.
- (3) Schrauzer, G.; Guth, T. *J. Am. Chem. Soc.* **1977**, *99*, 7189–7193.
- (4) Schrauzer, G. N. In *Energy Efficiency and Renewable Energy Through Nanotechnology*; Zang, L., Ed.; Springer: London, 2011; pp 601–623.
- (5) Dhar, N.; Seshacharyulu, E.; Biswas, N. *Proc. Natl. Acad. Sci., India* **1941**, *7*, 115–131.
- (6) Linnik, O.; Kisch, H. *Photochem. Photobiol. Sci.* **2006**, *5*, 938.
- (7) Hirakawa, H.; Hashimoto, M.; Shiraiishi, Y.; Hirai, T. *J. Am. Chem. Soc.* **2017**, *139*, 10929–10936.
- (8) Davies, J. A.; Boucher, D. L.; Edwards, J. G. *Advances in Photochemistry*; John Wiley & Sons, Inc.: New York, 1995; Vol. 19; pp 235–310.
- (9) Comer, B. M.; Medford, A. J. *ACS Sustainable Chem. Eng.* **2018**, *6*, 4648–4660.
- (10) Li, C.; Wang, T.; Zhao, Z.-J.; Yang, W.; Li, J.-F.; Li, A.; Yang, Z.; Ozin, G. A.; Gong, J. *Angew. Chem.* **2018**, *130*, 5376–5380.
- (11) Yang, J.; Guo, Y.; Jiang, R.; Qin, F.; Zhang, H.; Lu, W.; Wang, J.; Yu, J. C. *J. Am. Chem. Soc.* **2018**, *140*, 8497–8508.
- (12) Höskuldsson, A. B.; Abghoui, Y.; Gunnarsdóttir, A. B.; Skúlason, E. *ACS Sustainable Chem. Eng.* **2017**, *5*, 10327–10333.
- (13) Yuan, S.-J.; Chen, J.-J.; Lin, Z.-Q.; Li, W.-W.; Sheng, G.-P.; Yu, H.-Q. *Nat. Commun.* **2013**, *4*, 2249.
- (14) Larkins, F.; Lubenfeld, A. *J. Electron Spectrosc. Relat. Phenom.* **1979**, *15*, 137–144.
- (15) Chen, X.; Burda, C. *J. Phys. Chem. B* **2004**, *108*, 15446–15449.
- (16) Lazarus, M.; Sham, T. *Chem. Phys. Lett.* **1982**, *92*, 670–674.
- (17) Park, Y.; Kim, W.; Park, H.; Tachikawa, T.; Majima, T.; Choi, W. *Appl. Catal., B* **2009**, *91*, 355–361.
- (18) MacDonnell, F. M. *Proc. Natl. Acad. Sci. U. S. A.* **2018**, *115*, E557.
- (19) Göpel, W.; Anderson, J.; Frankel, D.; Jaehnic, M.; Phillips, K.; Schäfer, J.; Rucker, G. *Surf. Sci.* **1984**, *139*, 333–346.
- (20) Ketteler, G.; Yamamoto, S.; Bluhm, H.; Andersson, K.; Starr, D. E.; Ogletree, D. F.; Ogasawara, H.; Nilsson, A.; Salmeron, M. *J. Phys. Chem. C* **2007**, *111*, 8278–8282.
- (21) Barr, T. L.; Seal, S. J. *J. Vac. Sci. Technol., A* **1995**, *13*, 1239–1246.
- (22) Goldsmith, B. R.; Sanderson, E. D.; Bean, D.; Peters, B. *J. Chem. Phys.* **2013**, *138*, 204105.
- (23) Brigden, C. T.; Poulston, S.; Twigg, M. V.; Walker, A. P.; Wilkins, A. *J. Appl. Catal., B* **2001**, *32*, 63–71.
- (24) Tu, W.; Zhou, Y.; Zou, Z. *Adv. Mater.* **2014**, *26*, 4607–4626.
- (25) Kisch, H. In *Energy Efficiency and Renewable Energy Through Nanotechnology*; Zang, L., Ed.; Springer: London, 2011; pp 585–599.
- (26) Rusina, O.; Eremenko, A.; Frank, G.; Strunk, H. P.; Kisch, H. *Angew. Chem.* **2001**, *113*, 4115–4117.
- (27) Hellman, A.; Wang, B. *Inorganics* **2017**, *5*, 37.
- (28) Dimitrijevic, N. M.; Vijayan, B. K.; Poluektov, O. G.; Rajh, T.; Gray, K. A.; He, H.; Zapol, P. *J. Am. Chem. Soc.* **2011**, *133*, 3964–3971.
- (29) Anpo, M.; Yamashita, H.; Ichihashi, Y.; Ehara, S. *J. Electroanal. Chem.* **1995**, *396*, 21–26.
- (30) Yu, L.; Li, D. *Catal. Sci. Technol.* **2017**, *7*, 635–640.
- (31) van der Ham, C. J. M.; Koper, M. T. M.; Hetterscheid, D. G. H. *Chem. Soc. Rev.* **2014**, *43*, 5183.
- (32) Hirakawa, T.; Nosaka, Y. *Langmuir* **2002**, *18*, 3247–3254.
- (33) Li, X.-F.; Li, Q.-K.; Cheng, J.; Liu, L.; Yan, Q.; Wu, Y.; Zhang, X.-H.; Wang, Z.-Y.; Qiu, Q.; Luo, Y. *J. Am. Chem. Soc.* **2016**, *138*, 8706–8709.
- (34) Jeon, I. Y.; et al. *Sci. Rep.* **2013**, *3*, 1–7.